Monthly Notices
of the
ROYAL ASTRONOMICAL SOCIETY

MNRAS **502,** 3101–3112 (2021)
Advance Access publication 2021 January 29

doi:10.1093/mnras/stab242

GAMA/XXL: X-ray point sources in low-luminosity galaxies in the GAMA G02/XXL-N field

E. Nwaokoro,[1,2] S. Phillipps,[1]★ A. J. Young,[1] I. Baldry,[3] A. Bongiorno,[4] M. N. Bremer,[1] M. J. I. Brown,[5] L. Chiappetti,[6] R. De Propris,[7] S. P. Driver,[8] A. Elyiv,[9] S. Fotopoulou,[1] P. A. Giles,[10] A. M. Hopkins,[11] B. Maughan,[1] S. McGee,[12] F. Pacaud,[13] M. Pierre,[14] M. Plionis,[15] B. M. Poggianti[16] and C. Vignali[17,18]

[1]*Astrophysics Group, School of Physics, University of Bristol, Tyndall Avenue, Bristol BS8 1TL, UK*
[2]*Physics Department, Abia State University, Uturu, PMB 2000, Nigeria*
[3]*Astrophysics Research Institute, Liverpool John Moores University, IC2, Liverpool Science Park, 146 Brownlow Hill, Liverpool L3 5RF, UK*
[4]*INAF, Osservatorio Astronomico di Roma, via Frascati 33, I-00078 Monte Porzio Catone, Italy*
[5]*School of Physics and Astronomy, Monash University, Clayton, VIC 3800, Australia*
[6]*INAF, IASF Milano, via Corti 12, I-20133 Milano, Italy*
[7]*Finnish Centre for Astronomy with ESO, University of Turku, Vesilinnantie 5, FI-21400 Turku, Finland*
[8]*ICRAR, University of Western Australia, 35 Stirling Highway, Crawley, WA 6009, Australia*
[9]*Main Astronomical Observatory, National Academy of Sciences of Ukraine, 27 Akademika Zabolotnoho St, UA-04103 Kyiv, Ukraine*
[10]*Astronomy Centre, University of Sussex, Falmer, Brighton BN1 9QH, UK*
[11]*Australian Astronomical Optics, Macquarie University, 105 Delhi Road, North Ryde, NSW 2113, Australia*
[12]*School of Physics and Astronomy, University of Birmingham, Edgbaston, Birmingham B15 2TT, UK*
[13]*Argelander Institute für Astronomie, Universität Bonn, D-53121 Bonn, Germany*
[14]*AIM, CEA, CNRS, Université Paris-Saclay, Université Paris Diderot, Sorbonne Paris-Cité, F-91191 Gif-sur-Yvette, France*
[15]*Department of Physics, Aristotle University of Thessaloniki,Thessaloniki 54124, Greece*
[16]*INAF, Osservatorio Astronomico di Padova, vicolo dell'Osservatorio 5, I-35122 Padova, Italy*
[17]*Physics and Astronomy Department, Universitá di Bologna, via Gobetti 93/2, I-40129 Bologna, Italy*
[18]*INAF, Osservatorio di Astrofisica e Scienza dello Spazio di Bologna, via Gobetti 93/3, I-40129 Bologna, Italy*

Accepted 2021 January 26. Received 2021 January 20; in original form 2020 September 24

ABSTRACT

Relatively few X-ray sources are known that have low-mass galaxies as hosts. This is an important restriction on studies of active galactic nuclei (AGNs), hence black holes, and of X-ray binaries (XRBs) in low-mass galaxies; addressing it requires very large samples of both galaxies and X-ray sources. Here, we have matched the X-ray point sources found in the XXL-N field of the XXL survey (with an X-ray flux limit of $\sim 6 \times 10^{-15}$ erg s^{-1} cm^{-2} in the [0.5–2] keV band) to galaxies with redshifts from the Galaxy And Mass Assembly (GAMA) G02 survey field (down to a magnitude limit $r = 19.8$) in order to search for AGNs and XRBs in GAMA galaxies, particularly those of low optical luminosity or stellar mass (fainter than $M_r = -19$ or $M_* \lesssim 10^{9.5}$ M$_\odot$). Out of a total of 1200 low-mass galaxies in the overlap region, we find a total of 28 potential X-ray source hosts, though this includes possible background contaminants. From a combination of photometry (optical and infrared colours), positional information, and optical spectra, we deduce that most of the $\simeq$20 X-ray sources genuinely in low-mass galaxies are high-mass X-ray binaries in star-forming galaxies. None of the matched sources in a low-mass galaxy has a BPT classification as an AGN, and even ignoring this requirement, none passes both criteria of close match between the X-ray source position and optical galaxy centre (separation $\leq$3 arcsec) and high [O III] line luminosity (above $10^{40.3}$ erg s^{-1}).

Key words: galaxies: active – galaxies: star formation – X-rays: galaxies.

1 INTRODUCTION

Low optical luminosity galaxies known to contain active nuclei remain quite rare (Greene & Ho 2007; Gallo et al. 2008; Ho 2008; Pardo et al. 2016; Baldassare et al. 2017; Mezcua et al. 2018, and references therein). Such active nuclei are often searched for optically (e.g. Decarli et al. 2007; Reines, Greene & Geha 2013), but an alternative is to search at X-ray wavelengths (Gallo et al. 2008; Seth et al. 2008), which will also find non-AGN (active galactic nucleus) X-ray sources, again relatively rare in low-mass galaxies (e.g. Papadopoulou, Phillipps & Young 2016, and references therein). In order to explore this route, large X-ray surveys must be matched to deep spectroscopic surveys, as redshifts remain the key to determining the properties of the host galaxies.

★ E-mail: s.phillipps@bris.ac.uk

The XXL Survey (Pierre et al. 2016, hereafter XXL paper I) is the largest survey carried out with *XMM–Newton*, covering some 50 deg^2. One of the two XXL Survey fields, XXL-N, overlaps the field G02 of the Galaxy And Mass Assembly (GAMA) survey (Driver et al. 2011; Liske et al. 2015; Baldry et al. 2018) that has near-complete spectroscopic coverage of galaxies (including AGNs) in a total of five fields down to a magnitude limit of $r = 19.8$.

In this paper, we combine the two surveys. Specifically, we utilize the matched data for XXL point sources that have GAMA counterparts. We are therefore able to explore a sample of the lowest optical luminosity (hence mass) galaxies that are able to host X-ray detectable AGNs, or other potential point sources such as X-ray binaries (XRBs).

Section 2 describes the data used and details our sample selection from matching XXL and GAMA [originally Sloan Digital Sky Survey (SDSS)] objects. Section 3 then explores the properties of the matched objects, in particular the low optical luminosity galaxies with X-ray detections, and discusses whether the X-ray sources are likely AGNs or, instead, XRBs. Section 4 summarizes and discusses the results.

All optical magnitudes used in this work are in the AB system. In order to determine luminosity distances, and hence intrinsic properties, we use the GAMA standard cosmology with $H_0 = 70\,\mathrm{km\,s^{-1}\,Mpc^{-1}}$, $\Omega_\mathrm{m} = 0.3$, and $\Omega_\Lambda = 0.7$.

2 SAMPLE SELECTION

The GAMA survey is based on a highly complete galaxy redshift survey (Baldry et al. 2010, 2018; Driver et al. 2011; Hopkins et al. 2013; Liske et al. 2015) covering approximately 280 deg^2 to a main survey magnitude limit of $r = 19.8$. Galaxies were originally selected from SDSS images (Adelman-McCarthy et al. 2008; Abazajian et al. 2009; Aihara et al. 2011). The GAMA survey area is split into three equatorial (G09, G12, and G15) and two southern (G02 and G23) regions. In this work, we use galaxies from field G02, covering 55.7 deg^2, centred at RA $2^\mathrm{h}20^\mathrm{m}$, Dec. -7°. The input here came from SDSS data release 8 (DR8; Aihara et al. 2011).

The spectroscopic survey was undertaken with the AAOmega fibre-fed spectrograph (Saunders et al. 2004; Sharp et al. 2006) allied to the Two-degree Field (2dF) fibre positioner on the Anglo-Australian Telescope (Lewis et al. 2002). Across all the fields, it obtained redshifts for $\sim$300 000 targets covering $0 < z < 0.8$ (with a median redshift of $z \simeq 0.2$) with generally extremely high spatial completeness (Robotham et al. 2010). Baldry et al. (2018) summarize GAMA's third data release (DR3[1]), which includes the spectroscopy from the G02 field. Although the later addition of the G02 area to the survey meant that it is not as complete as the others, the 19.5 deg^2 subset, north of Dec. $= -6^\circ$ that overlaps with the XXL-N field (see below) does have redshift completeness of 95.5 per cent to the standard magnitude limit of $r = 19.8$ (21 000 objects).

XXL is the largest *XXM–Newton* survey to date (XXL paper I). It covered two 25 deg^2 areas over the energy range [0.5–10] keV. The northern field, XXL-N, is mostly covered by GAMA G02 data (see fig. 1 in Baldry et al. 2018). Observations were of 10 ks duration and reached a point source sensitivity of approximately 6×10^{-15} erg s^{-1} cm^{-2} in the [0.5–2] keV ('soft') band. A 'hard' band was defined to be [2–10] keV. The main aim of XXL was to survey galaxy clusters out to high redshift (Pacaud et al. 2016, hereafter XXL paper II). Giles et al. (2021) and Crossett et al. (2021) have also used matched GAMA G02 and XXL data to explore the X-ray emission from galaxy groups.

In addition, the overall survey has also detected more than 26 000 point sources (Chiappetti et al. 2018, hereafter XXL paper XXVII), which are expected to be nearly all AGN, at redshifts out to $z \sim 4$ (Fotopoulou et al. 2016b, XXL paper VI). (The AGN luminosity function from XXL has been discussed by Koulouridis et al. 2018, XXL paper XIX.) However, relatively few of the AGN are expected to be at the low redshifts required in order to study any low-luminosity hosts (see e.g. Fotopoulou et al. 2016a).

G02 and XXL-N additionally overlap with the CFHT Legacy Survey field CFHTLS-W1 (Gwyn 2012; Heymans et al. 2012). Links to other multiwavelength and spectroscopic data for objects in the XXL-N field are provided at the XXL website.[2]

The point sources in the northern field have been spatially linked to GAMA G02 galaxies by the GAMA/XXL Matching Group. The maximum allowable position difference between the X-ray and optical centroids was 10 arcsec, as in the construction of the 3XLSS source catalogue (XXL paper XXVII). This produced a sample of 1307 GAMA galaxies (GAMA internal catalogue XXLPointSourceCatv01) that is the basic sample from which we work. This catalogue contains the hard and soft band XXL flux measurements, derived from the raw count rates via a standard model (see e.g. XXL paper XXVII, section 2.1).

We matched this to the public GAMA file G02TilingCatv07 that contains basic information on the GAMA galaxies in G02 for which spectroscopy was attempted (including extinction corrected r-band magnitudes down to $r \simeq 20$ from SDSS and/or CFHTLS). We extracted those with successful observations with GAMA redshift quality $nQ > 2$ (i.e. 'science quality' redshifts; see Liske et al. 2015 for details). This gives 806 galaxies with secure redshifts and with X-ray detections, about 4 per cent of the GAMA galaxies in the overlap region, consistent with the fraction of AGN seen elsewhere in GAMA (e.g. Yao et al. 2020). Restricting our sample to sources with at least 10 counts in the soft X-ray band (0.5 to 2 keV), in order to allow moderately good estimates of the X-ray fluxes, reduces this to 712. Of these, 676[3] have *ugriz* photometry in the input catalogue and emission line measurements from the GAMA spectra.

3 THE MATCHED GALAXIES

For orientation, Fig. 1 shows the distribution of the X-ray point sources in terms of their redshifts z and host galaxy absolute r-band optical magnitudes M_r. Specifically, we utilize here the SDSS ModelMag to obtain M_r. Objects are detected to $z \simeq 0.8$, but of course low-luminosity galaxies have to be much closer. If we choose $M_r = -19$ as our 'low luminosity' limit, there are just 28 objects, with $z \leq 0.14$ (all bar one below $z = 0.1$; see bottom panel in the figure). Of these, a small number of matches are likely to be chance alignments of a low-luminosity galaxy and a distant AGN (as discussed in Section 3.2.1, below), so 28 is likely to be an upper limit to genuine matches. This is out of a total of about 1200 GAMA galaxies to this absolute magnitude limit in the XXL-N overlap region, emphasizing the low probability of finding sufficiently bright X-ray sources in optically faint galaxies.

For simplicity, and to avoid confusion between low optical luminosity and low X-ray luminosity, we refer to this sample of

[1] www.gama-survey.org/dr3/

[2] See xxlmultiwave.pbworks.com/w/page/54609468/FrontPage

[3] We have removed a handful of objects that were fragments of larger galaxies and therefore had spurious photometry.

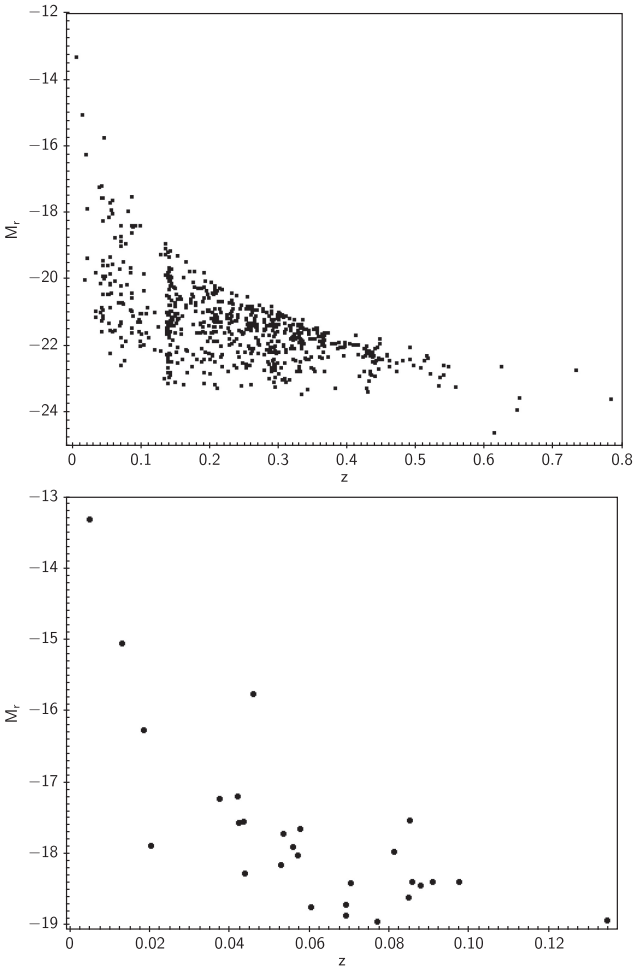

Figure 1. Plot of absolute r-band magnitude M_r for the 676 GAMA/G02 galaxies matched to XXL sources (with at least 10 soft band counts; see text) against redshift z. Lower panel: Expanded version showing only the 28 GAMA galaxies fainter than $M_r = -19$ (the 'low-mass' sample).

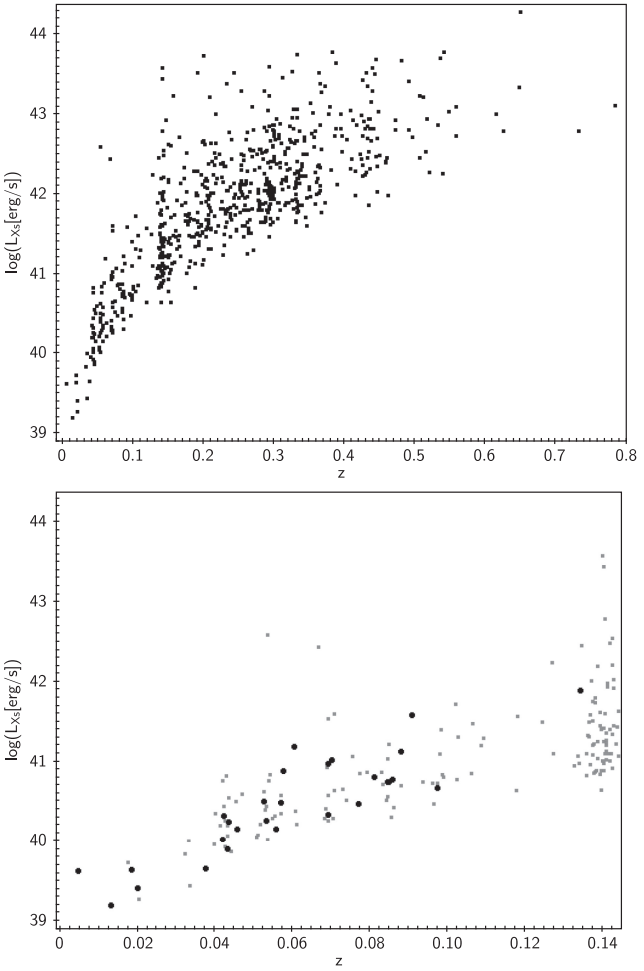

Figure 2. Plot of soft-band X-ray luminosity L_{Xs} against redshift z for the same objects as in Fig. 1. Lower panel: Expanded version showing only the galaxies at redshifts out to $z = 0.145$, approximately the limit for our low-mass sample. The latter are shown as filled circles.

28 objects as 'low-mass' galaxies hereafter. At and below $M_r = -19$ most of the galaxies are relatively blue (Baldry et al. 2012) so with a standard mass-to-light conversion (e.g. Bell et al. 2003; Kauffmann et al. 2003a), we expect the galaxies with $M_r = -19$ to correspond approximately to a stellar mass of $10^{9.5}$ $M_\odot$ (with a scatter of around ± 0.15 dex). Red galaxies will be slightly more massive while, conversely, any galaxies with a significant contribution to the (r-band) flux from an AGN may have lower stellar masses.

Fig. 2 similarly shows the soft-band X-ray luminosities of the matched objects. Here, we have simply used the catalogued XXL fluxes in each band and the luminosity distances to derive generic luminosities which we refer to as L_{Xs} (soft band) and L_{Xh} (hard band). We have not attempted to make any corrections to the X-ray data for spectral shape or redshift. Nearby galaxies are detected down to $L_{Xs} \simeq 10^{39}$–10^{40} erg s^{-1}, while the most luminous (more distant) sources are at around $10^{43.5}$ erg s^{-1}. The brightest source apparently in a low-mass galaxy has $L_{Xs} \simeq 10^{42}$ erg s^{-1} (but see Section 4).

Interestingly, from the lower panel, we can see that the X-ray luminosities are essentially the same, at a given (low) z, in both the brighter galaxies ($M_r < -19$) and the low-mass sample. If we look at this in another way, as in Fig. 3, this means that there is a very wide range of optical luminosities at a given X-ray luminosity, particularly in the range $L_{Xs} < 10^{42}$ erg s^{-1} that is sampled in our low mass, low redshift sub-sample.

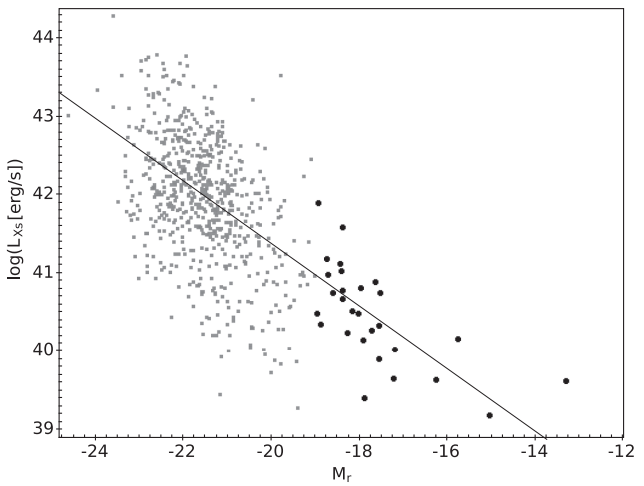

Figure 3. Plot of soft-band X-ray luminosity L_{Xs} against absolute r-band magnitude M_r for the same objects as in Fig. 2. Low-mass galaxies are again the filled circles. The line indicates the approximate locus of AGN with an Eddington ratio of 10^{-2} (see text).

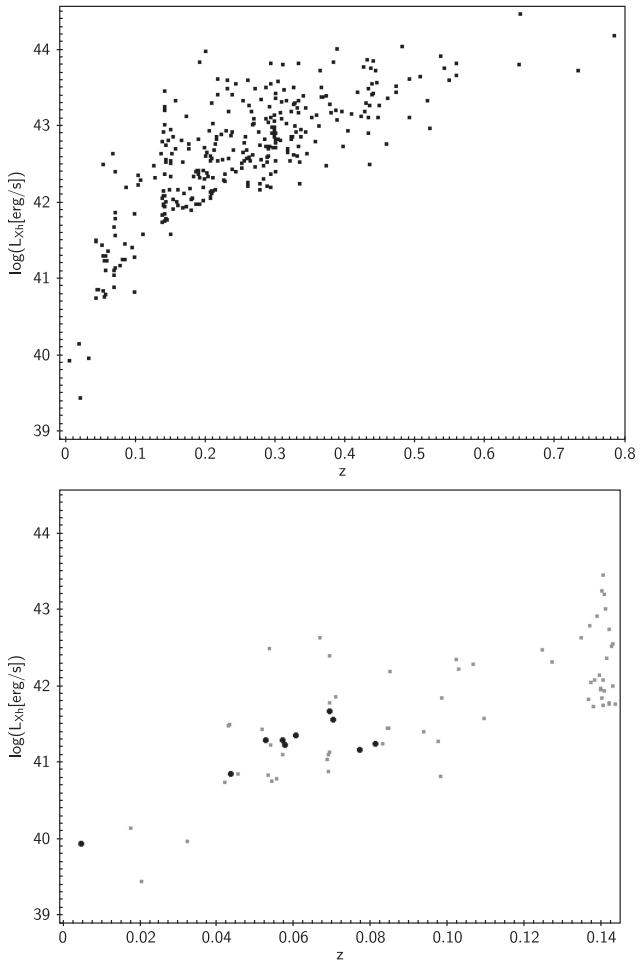

Figure 4. As Fig. 2 but for the hard X-ray band detected objects.

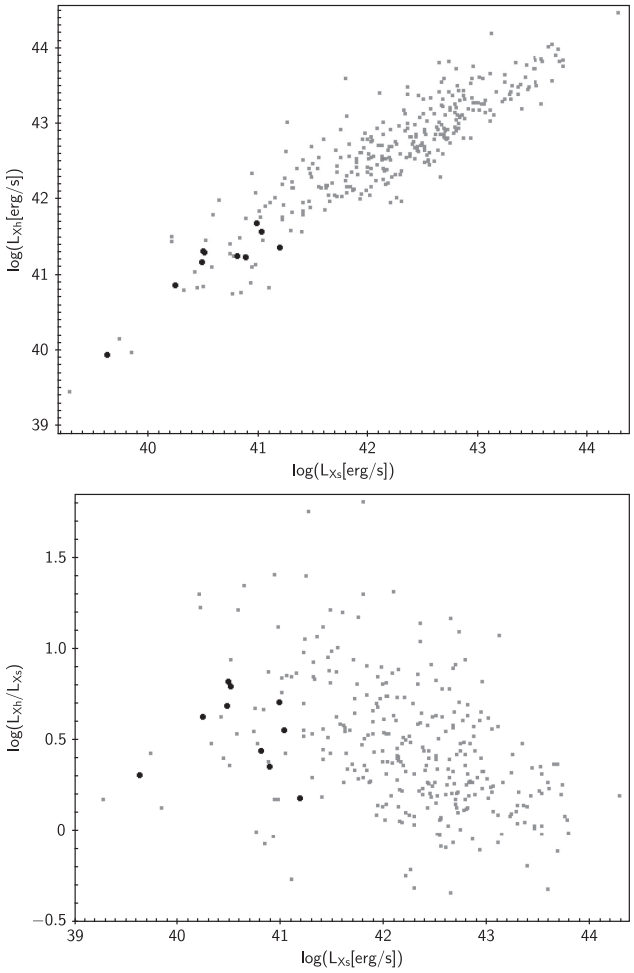

Figure 5. As Fig. 3 but for L_{Xs} versus L_{Xh} for sources detected in both bands. The bottom panel shows the ratio L_{Xh}/L_{Xs}. Low-mass galaxies shown as filled circles as before.

Far fewer objects (320) meet the same criterion of at least 10 counts in the hard band, but for completeness, the available hard-band luminosities L_{Xh} are plotted against redshift in Fig. 4. We find L_{Xh} of the order of 10^{42} down to $10^{39.5}$ erg s^{-1} for the nearby sources (bottom panel), while the brighter, more distant ones range up to around 10^{44} erg s^{-1} (top panel). Unfortunately, only 10 of the low-mass sample have hard X-ray counterparts with 10 or more counts, but we can note that, as for the soft X-ray detections, they share the same range of X-ray luminosities as the luminous optical galaxies at the same redshifts.

The hard-band luminosity is plotted against the soft-band luminosity, for objects with at least 10 counts in both bands, in Fig. 5. Though with significant scatter, typically $L_{Xh}/L_{Xs} \sim 10^{0.5}$ for both the low and high-optical luminosity galaxies, though this decreases somewhat, to around $10^{0.2}$, at high X-ray fluxes (sampled only by the high-optical luminosity sources) as shown in the bottom panel. The range of L_{Xh}/L_{Xs} seen is consistent with that observed for XXL point sources in general (XXL paper XXVII).

3.1 The X-ray sources

From the previous figures, it is evident that the low-mass sample galaxies contain relatively low X-ray luminosity XXL sources. This could reasonably be because lower stellar mass galaxies contain lower mass central supermassive black holes (SMBHs) and therefore generate relatively low fluxes even when the BH is active. If we assume that our galaxies with $-19 < M_r < -13$ (i.e. stellar mass $M_* \sim 10^{9.5}$ to 10^7 M$_\odot$) follow the same type of Magorrian et al. (1998) relation between galaxy stellar mass and SMBH mass $M_{\rm bh}$ (e.g. Ferrarese et al. 2006a, b; Baldassare et al. 2020) as do larger galaxies, then we can expect values of $M_{\rm bh}$ of the order of $10^{6.8}$ to $10^{4.3}$ M$_\odot$ (Gallo et al. 2008; Reines et al. 2013). Observations of a small number of such objects (e.g. Dudik et al. 2005; Panessa et al. 2006) suggest that such low-mass SMBH should correspond, with a large spread, to hard X-ray luminosities $L_{Xh} \sim 10^{42}$ to 10^{37} erg s^{-1}. The upper end of this range is compatible with the values in our, also rather limited, hard X-ray detected low-mass sample from Fig. 4 (filled circles): we would be unable to detect sources at the lower end. In the better defined Fig. 2 (lower panel) for the soft X-ray detected objects, the similar upper envelopes for the high and low-mass objects may likely be a selection effect due to the decreasing chance of finding higher X-ray luminosity sources in the rather small volumes sampled at lower z.

If they are AGN, the similarity between the X-ray fluxes for the sources in low-mass galaxies and those in more luminous galaxies at the same redshift (which should have more massive SMBH) would then be accounted for by differences in their Eddington ratios. Given that $M_r = -19$ corresponds to about $M_{\rm bh} \sim 10^{6.8}$ M$_\odot$, $L_{\rm Edd} \sim 10^{45}$ erg s^{-1}. At this M_r, L_{Xh} is typically $\sim 10^{41.5}$ erg s^{-1} (and $L_{Xs} \sim 10^{41}$ erg s^{-1}), so allowing for a bolometric correction to L_{Xh} of a

factor 30 as in Panessa et al. (2006), $L_{\rm bol} \sim 10^{43}$ erg s^{-1}, i.e. $L_{\rm bol}/L_{\rm Edd} \sim 10^{-2}$. In fact, looking at the whole data set in Fig. 3 for L_{Xs}, if we assume that $L_{\rm Edd}$ scales linearly with stellar luminosity, the bulk of the data for both high and low-mass samples is roughly centred on this typical Eddington ratio of around 10^{-2}, as shown by the solid line. This is in agreement with the values found by Panessa et al. (2006) for Seyfert galaxies with similar mass black holes (see their fig. 7) and the peak of the Eddington ratio distribution suggested by Alexander & Hickox (2012) for optically selected AGN. The roughly diagonal upper and lower envelopes in Fig. 3 then reflect the maximum and minimum Eddington ratios in the sample, $\sim 10^{-1}$ and $\sim 10^{-4}$, respectively, similar to the range in Panessa et al. (2006) for Type 1 AGN. Panessa et al. and Ho (2008) also note that low-luminosity AGN (LLAGN) mostly have Eddington ratios $<10^{-2}$.

Thus, in terms of their luminosities, and the various correlations shown, the X-ray sources we see in the low-mass galaxies *could* be AGN powered by correspondingly low-mass BH. Such systems, effectively intermediate mass black holes (cf. Koliopanos et al. 2017), are important for the clues they may provide to the seeding mechanism of SMBH in the early Universe; see e.g. the reviews of Mezcua (2017) and Woods et al. (2019).

However, we should also consider the alternative that the X-ray sources seen at low redshift (in both optically bright and faint galaxies) are not AGN but stellar sources, either high-mass X-ray binaries (HMXB) or low-mass X-ray binaries (LMXB). HMXBs come from short-lived stars and therefore reflect recent star formation activity (Grimm, Gilfanov & Sunyaev 2003; Ranalli, Comastri & Setti 2003; Mineo, Gilfanov & Sunyaev 2012). In the [2–10] keV hard band, Ranalli et al., for instance, found the X-ray emission in star-forming galaxies to follow $L_{Xh} \simeq$ SFR (in M$_\odot$ yr^{-1}) $\times\ 10^{39.7}$ erg s^{-1}. LMXBs, on the other hand, are found in old stellar populations (Boroson et al. 2011) and their combined X-ray luminosity reflects the total stellar mass of their host galaxy: Gilfanov (2004) suggests $L_X \simeq 10^{29} M_*/{\rm M}_\odot$ erg s^{-1}. In both cases, the brighter examples exceed 10^{39} erg s^{-1} so can potentially be seen in our low z sample. Papadopoulou et al. (2016) have previously found Chandra X-ray sources at these luminosities both in dwarf elliptical galaxies in the Virgo Cluster (presumed to be LMXBs) and in nearby star-forming dwarf irregular galaxies (presumably HMXBs). At the highest individual luminosities are the ultra-luminous X-ray (ULX) sources (Grimm et al. 2003) that extend the HMXB range from about 10^{40} to 10^{41} erg s^{-1}. These are found in strongly star-forming galaxies, including in some low-mass star-forming galaxies (Grisé et al. 2011; Swartz et al. 2011). Sutton et al. (2012) discuss a number of extreme sources above 10^{41} erg s^{-1} that may have a different origin to lower luminosity XRBs.

It should be noted, when considering the X-ray luminosities, that there will be two regimes. In giant galaxies or strongly star-forming galaxies, there may be many individual XRBs, but at the resolution of our XXL observations, compared to the extent of our faint galaxies, these will generally be observed as a single source with the summed luminosity of all the XRBs therein. On the other hand, in detectable dwarf galaxies of low stellar content and low star formation rate we expect the X-ray flux to be (mostly) from a single bright XRB.

It is of interest at this point to briefly consider the host galaxies of the X-ray sources. Fig. 6 shows the k-corrected $(g-r)$ versus M_r colour–magnitude diagram for the matched GAMA galaxies (again using the SDSS ModelMags). Typical magnitude and colour errors are 0.02 and 0.03 magnitudes, respectively. Excluding two faint objects with apparently extremely red colours [off the scale at $(g-r) > 1$],[4] the distribution in the optical colour–magnitude diagram of the current low-mass sample is consistent with that seen in GAMA low redshift, low-luminosity galaxies as a whole (e.g. Baldry et al. 2012). A handful of the low-mass sample may possibly occupy the low-luminosity tail of the red sequence at $(g-r) \simeq 0.6-0.7$, but the majority are evidently blue cloud galaxies, bluer than $(g-r) \simeq 0.5$ [though we should caution that for the fainter galaxies SDSS colour errors may be large enough ($\simeq$0.1) to somewhat blur the division; in addition, we have not attempted any correction for internal reddening]. If the X-ray sources are not AGN, then the host galaxy colours suggest that they should be primarily HMXBs in star-forming galaxies (though of course LMXBs may possibly occur in the old stellar population in the bulges of such galaxies).

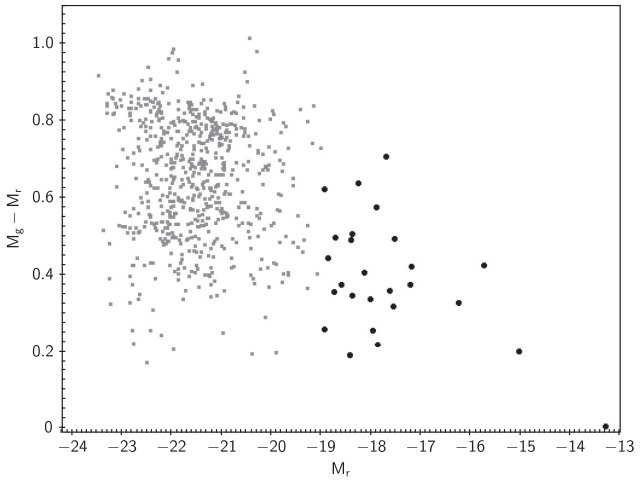

Figure 6. K-corrected $(g-r)$ versus M_r colour–magnitude diagram for all sample galaxies. As in the previous figures, sources in the low-mass sample are the filled circles.

In terms of their environment, only one of the low-mass sample, GAMA J022544.79–054106.2, is a member of what could be considered a cluster (the X-ray cluster XLSSC 054; see XXL paper II), with a GAMA friends-of-friends count $N_{\rm fof}$ of 54 neighbours (Robotham et al. 2011). Even then, it is an outlying member, 14 arcmin ($\simeq$0.9 Mpc) from the central galaxy. This object does not stand out in any way compared to the other matched X-ray sources in Table 1. A quarter (7/28) of the final matched low-mass sample galaxies are members of groups with $3 \leq N_{\rm fof} \leq 8$, consistent with the fraction (20 per cent) for all low-mass GAMA galaxies in G02, and the rest are isolated or paired galaxies. Thus, environmentally the host galaxies are again consistent with being typical low-mass star-forming galaxies, which preferentially occupy small groups and other sparse environments.

3.2 AGN or XRBs?

3.2.1 Positions

There are a number of ways in which we can hope to determine which, if any, of our sources (apparently) in low-mass galaxies are AGN. Perhaps the most obvious is to look at their positions within the host galaxies. XXL positions, relative to SDSS, for convincing matches should be good to about 5 arcsec (cf. Pineau et al. 2011,

[4]They have a measured $g > 21$ and neither actually makes our final sample as they are close on the sky to unrelated AGN (see Section 4).

Table 1. Low-mass galaxy X-ray detections.

GAMA ID	3XLSS ID	z	M_r	s arcsec	r kpc	$\log(L_{Xs})$ erg s^{-1}	$\log(L_{Xh})$ erg s^{-1}	$\log(L_{[O\,III]})$ erg s^{-1}	$\log(L_{H\,\alpha})$ erg s^{-1}	Class
J021657.27–055740.4	J021657.9–055741	0.042	−17.6	9.9	8.2	40.3	–	39.9	40.2	SF/BQ
J021748.49–044410.1	J021748.3–044410	0.038	−17.2	2.8	2.1	39.7	–	40.1	40.1	SF
J021921.56–040222.3	J021921.8–042214	0.042	−17.2	8.6	7.1	40.0	–	39.1	39.6	–
J021007.68–050508.7	J021007.7–050500	0.060	−18.7	8.0	9.4	41.2	41.4	40.3	40.7	SF/BQ
J021122.14–044757.1	J021122.4–044756	0.088	−18.4	4.5	7.4	41.1	–	40.7	40.6	SF
J021142.86–044804.9	J021142.7–044812	0.070	−18.4	7.6	10.2	41.0	41.6	39.2:	40.1	–/BQ?
J020928.67–041616.6	J020929.2–041620	0.058	−17.6	8.7	9.7	40.9	41.2	39.9:	40.2	–/BQ
J020747.54–054805.7	J020747.3–054809	0.043	−17.5	4.7	4.0	39.9	–	39.4	39.7	–
J020800.90–054717.2	J020800.9–054708	0.044	−18.3	8.6	7.4	40.2	40.9	37.4:	39.5	–
J020356.03–053545.8	J020356.1–053545	0.019	−16.3	2.3	0.9	39.6	–	39.3	39.4	SF
J020427.48–045840.2	J020427.0–045845	0.013	−15.0	7.7	2.1	39.2	–	39.6	39.8	SF
J020301.04–045105.9	J020301.5–045104	0.135	−18.9	7.5	17.9	41.9	–	40.2	40.5	SF/BQ?
J022219.36–052043.2	J022219.2–052047	0.085	−18.6	4.7	7.5	40.8	–	39.4	40.5	SF
J022147.87–044613.3	J022147.9–044613	0.020	−17.9	1.3	0.5	39.4	–	40.8	40.8	SF
J022127.57–043403.3	J022127.9–043408	0.085	−17.5	8.0	12.7	40.8	–	39.7	40.0	SF/BG?
J022336.83–042834.0	J022337.0–042827	0.069	−18.9	7.4	9.8	40.3	–	40.1	40.6	SF
J022544.79–054106.2	J022544.8–054104	0.053	−17.7	1.7	1.8	40.3	–	39.1	–	–
J022654.22–052555.3	J022654.4–052602	0.046	−15.7	8.0	7.2	40.2	–	39.5	39.4	SF
J022736.40–050815.1	J022736.6–050817	0.077	−18.9	4.2	6.2	40.5	41.2	40.6	40.9	SF
J022858.99–050447.6	J022858.9–050449	0.056	−17.9	1.8	1.9	40.2	–	–	–	P
J021528.65–034932.1	J021529.1–034937	0.069	−18.7	8.9	11.8	41.0	41.7	40.1	40.4	–
J020922.52–051808.2	J020922.7–051813	0.091	−18.4	6.7	11.3	41.6	–	39.0:	40.4	–/BG?
J020455.30–040433.8	J020455.1–040426	0.053	−18.1	8.0	8.2	40.5	41.3	–	40.1	–
J020237.61–061434.4	J020237.6–061435	0.005	−13.3	1.5	0.1	39.6	39.9	38.4	38.5	SF
J020414.13–050926.8	J020414.0–050935	0.086	−18.4	9.2	14.8	40.8	–	39.9	40.0	SF
J022109.87–044544.5	J022109.7–044544	0.098	−18.4	1.3	2.4	40.7	–	40.3	40.7	SF
J023129.75–044831.2	J023129.9–044824	0.081	−18.0	7.2	11.0	40.8	41.3	40.2	40.4	SF
J023425.55–041105.8	J023425.4–041113	0.057	−18.0	7.5	8.3	40.5	41.3	40.4	40.3	SF

Notes. In columns 5 and 6, s and r are the angular separation and projected linear separation between the GAMA and XXL positions. Galaxies marked with a dash in the emission line columns have zero or negative fluxes and those values marked with a colon have large errors (S/N below 2). The remainder have errors less than 0.1 dex. In the 'Class' column, a dash means no BPT classification (not all required lines measured), P is for a passive galaxy with no measured lines. Qualifiers /BQ, /BQ?, /BG? indicate likely background contaminants, as described in the text.

XXL paper XXVII) while we have a maximum matching radius of 10 arcsec. Fig. 7, which plots the separation s between the XXL and SDSS positions, bears out this expectation with a strong peak between zero and 4 arcsec with a tail to 10 arcsec in the overall distribution (grey histogram in the bottom panel). In both panels, we see that the relatively low X-ray luminosity sources in the low-mass galaxies are often in the 6 arcsec to 10 arcsec range, implying that these are less likely to be nuclear sources. On the other hand, the more distant, high X-ray luminosity sources ($L_{Xs} \gtrsim 10^{42.5}$ erg s^{-1}) are generally at low separations (<4 arcsec), indicating likely genuine central sources, i.e. AGN as expected for these strong point sources.

However, 11 of the sources in low-mass galaxies do have separations less than 5 arcsec (7 less than 3 arcsec) so are spatially compatible with being AGN. Physically, this rough dividing line at $s = 5$ arcsec corresponds to galactocentric distances r between 1 and 12 kpc for galaxies between $z = 0.01$ and 0.14 (see Fig. 8). The top panel emphasizes that a significant fraction of the low-mass sample lies close to the upper allowed galactocentric distance at any z.

Given this last point, we should check whether our sample may be contaminated by unconnected (background) sources, particularly at the larger radial separations between the GAMA galaxy and the XXL source position. We can estimate that XXL has a surface density of around 500 AGN per square degree (XXL paper XXVII), so the expected number in a circle of radius 10 arcsec centred on a random point will be about 0.01. We have 20 000 GAMA galaxies in the well sampled overlap region, so we could generally expect around 200 interlopers in the 1307 GAMA matches, i.e. a contamination fraction around 15 per cent. This would scale to 27 spurious matches in the 176 low-redshift objects plotted in the top panel of Fig. 8 at $z < 0.145$, including about 4 in the low-mass sample. These would of course be mostly at the larger separations: within the 5 arcsec radius we tentatively proposed for plausible nuclear sources we would expect only 4 per cent contamination, i.e. 4 spurious matches in a total of 105 low z galaxies with $s < 5$ arcsec. Thus, it seems that while a few of the low-mass sample with large separations may not be genuine associations, the large majority should be real. At low separations essentially all the 11 low-mass matches should be real.

In fact, as we discuss in Section 4, three of the low-mass galaxies with large separations from the XXL position do have known quasars within 10 arcsec of the GAMA position. In two further cases, given the relatively large uncertainty, the XXL position is also compatible with that of a known QSO beyond the 10 arcsec circle from the galaxy, suggesting that 4 or 5 is indeed a reasonable estimate for the number of contaminants in the low-mass sample.

Another reality check can be obtained by looking at the typical sizes of low-mass galaxies. From the GAMA survey itself (Lange et al. 2015, 2016), low redshift, low-mass galaxies have effective radii in a range up to ∼7 kpc at stellar masses $\simeq 10^{9.5}$ M$_\odot$ corresponding to $M_r = -19$ (in agreement with the *HST* based study of van der Wel et al. 2014), the upper limit decreasing to ∼3 kpc at 10^8 M$_\odot$ ($M_r \sim -15$). Thus, if we take the overall size to be $\simeq 3 r_{\rm eff}$ [which contains ≃90–95 per cent of the light, hence stars, for any reasonable radial profile (Graham & Driver 2005)], then this gives us galaxy radii up to ∼20 kpc for $M_r = -19$ and 12 kpc for $M_r = -15$, which are

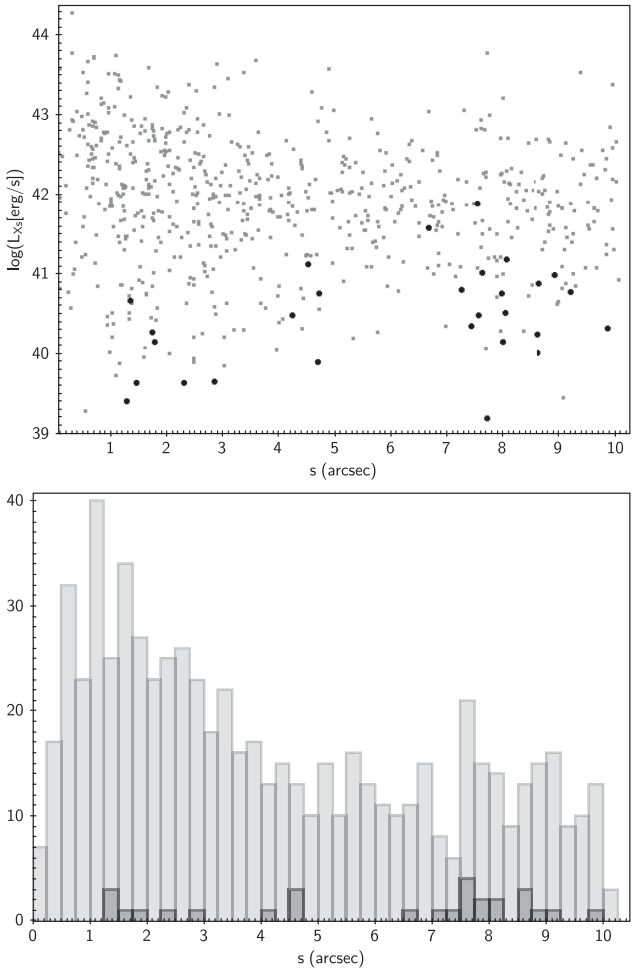

Figure 7. Distribution of angular separations s (in arcsec) between the GAMA (SDSS) and XXL positions for the soft X-ray selected sample. As in the previous figures, sources in low-mass galaxies are the filled circles. The bottom panel shows the histogram of the separations for the whole sample (grey) and the low-mass sample (black).

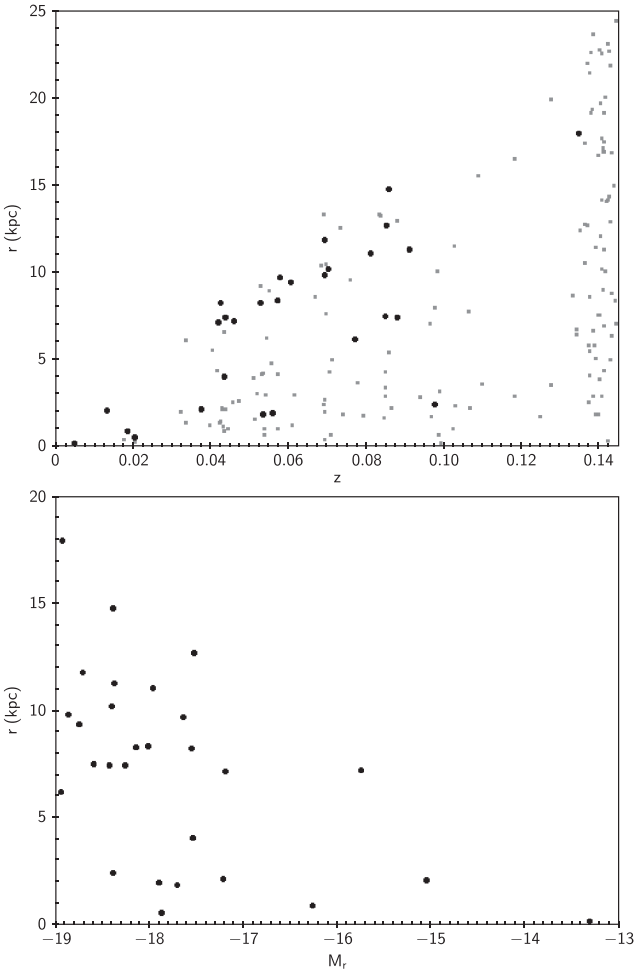

Figure 8. Top panel: Distribution of physical separations r (in kpc at the galaxy redshift) between the GAMA (SDSS) and XXL positions for the soft X-ray selected galaxies with $z < 0.145$. Sources in low-mass galaxies are the filled circles. Bottom panel: Galactocentric distance r of the XXL source, relative to the GAMA galaxy centroid, versus the host galaxy's absolute magnitude, for the low-mass sample.

sufficient to contain the galactocentric separations seen in the bottom panel of Fig. 8. Hence, again, it is entirely plausible that the majority of the matches between low-mass galaxies and XXL sources are genuine.

3.2.2 Spectral classification

As, by definition, our sample objects have spectra, we can search for evidence of AGN via any detected spectral lines. The [O III] λ5007 line is often used as an indicator of optical AGN power (Heckman et al. 2005), including specifically for GAMA galaxies (Gordon et al. 2017), and is also observed from the interstellar medium (ISM) of star-forming galaxies (e.g. Kennicutt 1992; Kauffmann et al. 2003b). First, in Fig. 9 (top panel), we plot the [O III] λ5007 line luminosities, $L_{\rm O\,III}$, for the 494 objects from our complete sample (including 26 of the low-mass subset) that have detectable [O III] emission line fluxes, against their soft X-ray luminosities. We can see that there is a general, though very broad, trend for high X-ray luminosity to correlate with high [O III] line luminosity (Mulchaey et al. 1994). This is clearer above $L_{\rm O\,III} \simeq 10^{41.5}$ erg s^{-1}, which Gordon et al. (2017) classify as the regime of high-luminosity AGN (see also Panessa et al. 2006).

The large majority of the low-mass galaxies, though, have $L_{\rm O\,III} \lesssim 10^{41}$ erg s^{-1}, where there is no correlation. This might be expected to be the case if the X-ray sources are individual HMXBs in star-forming galaxies of varied SFRs and ISM conditions (and hence emission line fluxes; Kennicutt 1992). This is supported by the more luminous optical galaxies at low-redshift typically having similar X-ray luminosities but higher [O III] luminosities than the low-mass galaxies.

The middle panel of Fig. 9 shows the corresponding plot for the H α line luminosity,[5] a standard proxy for star formation rate (Kennicutt 1994). At low L_{Xs}, there is little correlation of L_{Xs} with $L_{\rm H\,\alpha}$, again suggesting that at low L_{Xs} we see individual HMXB luminosities (in particular in the low-mass galaxies) while the H α measures the integrated SFR. For the more powerful sources (at $L_{Xs} \gtrsim 10^{41}$), the weak correlation seen presumably arises because L_{Xs} now measures the integrated luminosity of multiple HMXBs in the galaxies with high star formation rates (e.g. Grimm et al. 2003).

[5]The GAMA spectroscopic resolution of ∼1600 in the red (Hopkins et al. 2013) is sufficient to separate H α from the N II lines.

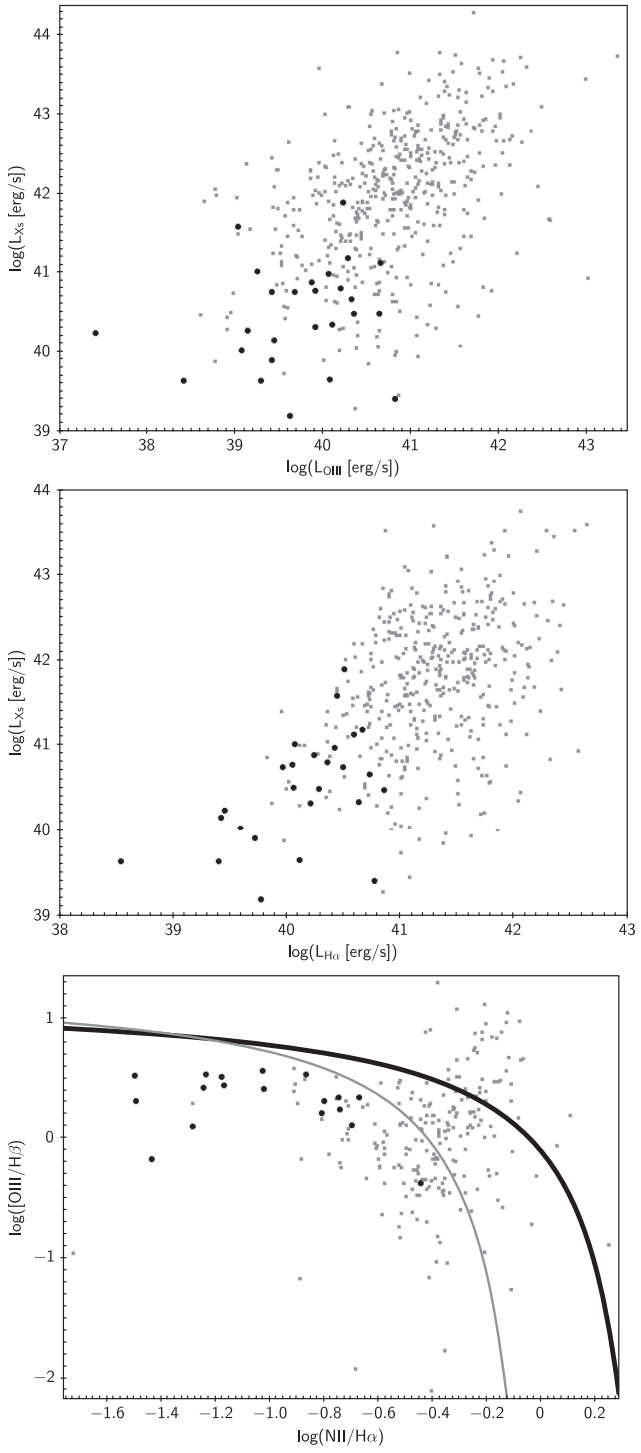

Figure 9. Top: Comparison of soft X-ray and [O III] λ5007 line luminosities for the 494 galaxies in our overall sample with detectable [O III] emission. The 26 low-mass galaxies with [O III] line measurements are shown by filled circles. Middle: Same except for H α luminosity (440 objects, again including 26 low-mass galaxies). Bottom: Standard BPT diagram for the 346 emission line galaxies in our sample that have all four required lines measured, including 20 from the low-mass sample. The lines are the Kewley (thick, upper) and Kauffmann (thin, lower) demarcation lines between AGN and star-forming galaxies. The area between the lines is commonly assumed to be occupied by composite systems.

Only one low-mass galaxy in our sample has neither measurable H α nor [O III] emission lines, implying at most one passive low-mass system hosting an X-ray source, potentially an LMXB).

The bottom panel of Fig. 9 then shows a standard BPT diagram (Baldwin, Phillips & Terlevich 1981), used to distinguish star-forming galaxies from AGN. Here we are, of course, limited to galaxies with detections in each of the four required lines H α, H β, [O III] λ5007 and [N II] λ6583 (346 objects, 18 in the low-mass sample). We have made the standard GAMA correction to the Balmer line fluxes for underlying absorption in the stellar continuum (as in Hopkins et al. 2013; Gordon et al. 2017), by multiplying by a factor (EW+2.5)/EW, where EW is the line equivalent width in Å. Full details of the emission-line measurement process in GAMA are given in Hopkins et al. (2013).

It is evident that while high-mass galaxies extend well into the AGN area as defined by Kewley et al. (2001) above the thick line (as expected by comparison with the GAMA data of Gordon et al. 2017, their fig. 4), this is not the case for the low-mass sample (filled circles).

The region between the Kewley line (higher curve) and the corresponding (lower, thin) line according to Kauffmann et al. (2003b) is usually assigned to composite objects with both an AGN and star formation, and we can see that no low-mass galaxies lie in this area, either.

The 18 BPT-classified low-mass galaxies are thus all in the star-forming region, with nine other objects not having all the required lines measured, though they do have measurable H α, or in one case just the [O III] line (Fig. 9, top and middle panels). We might therefore presume that the extra nine sources are also star-forming galaxies. Thus from the spectral line information, we could have up to 27 star-forming galaxies, although up to nine of these could still be AGN with relatively weak or poorly measured lines (cf. Miller et al. 2003; Agostino & Salim 2019), though see the next subsection for evidence against this. We also have one likely passive galaxy. We revisit these numbers in the light of possible contaminants in Section 4.

3.2.3 *Mid-infrared colours*

Another useful discriminant between AGN and star-forming galaxies is the mid-infrared colour. Specifically looking at the *WISE* 3.4 micron (W1) and 4.6 micron (W2) bands, Stern et al. (2012) suggest a simple division at W1–W2 = 0.8,[6] with ≃80 per cent of AGN having redder colours (see also Jarrett et al. 2011; Yao et al. 2020), though see the caveat in Hainline et al. (2016) regarding dwarf galaxy colours. Passive galaxies typically have $0 \lesssim$ W1–W2 $\lesssim 0.3$ and star-forming galaxies $0 \lesssim$ W1–W2 $\lesssim 0.6$ (Cluver et al. 2014). None of the low-mass sample galaxies has W1–W2 > 0.8. One, with photometry possibly affected by a nearby quasar (see below), has W1–W2 $\simeq 0.7$, while the passive galaxy has W1–W2 $\simeq 0.6$ (though with an error ≃0.2). The rest have W1–W2 $\lesssim 0.3$. Thus again, we have no significant evidence for any AGN in the low-mass sample.

4 DISCUSSION AND SUMMARY

From our initial sample of matched XXL point sources and GAMA galaxies, 28 were classed as 'low mass'; though strictly this sample was limited by r-band absolute magnitude, at $M_R = -19$, this translates approximately to a stellar mass limit of $10^{9.5}$ M$_\odot$. Because of the depth of the GAMA spectroscopic survey, these all lie at

[6]Note that *WISE* magnitudes are on the Vega not AB system.

redshifts below $z = 0.145$ (and all except one are at $z < 0.1$). These 28 sources are listed in Table 1 with their key X-ray and optical properties.

In terms of the host galaxies, from the optical colour–magnitude diagram, there are possibly a handful of fairly 'red' galaxies, but the large majority of X-ray sources in low-mass hosts are clearly associated with 'blue cloud' galaxies. Only one of the low-mass galaxies lies in a rich group or small cluster, the remainder are isolated or in small groups with no more than eight members.

The matched low-mass objects have an apparent range of X-ray luminosities from 10^{39} to 10^{42} erg s^{-1}, similar to those of sources in higher optical luminosity galaxies at the same redshifts and compatible with any of the likely sources, viz. (lowish mass) SMBH, HMXB, or LMXB, except that we do not expect HMXBs or LMXBs to extend to the highest X-ray luminosities that we find (though ULXs do). Of course, it is possible that the highest luminosity sources contain more than one bright HMXB, say, though the probability of this is low in a low mass, low star formation rate system (see below).

Positionally, the maximum matching radius is 10 arcsec, while the XXL position uncertainty is expected to range up to around 5 arcsec. On these grounds, 11 of the low-mass sample could well host central sources (position mismatch <5 arcsec). However, this uncertainty corresponds to between about 1 and 10 kpc at the distances of the galaxies, so non-central sources are certainly plausible, too.

Statistically, contamination from non-associated background AGN may account for 4 or 5 of the 28 low-mass galaxy matches out to 10 arcsec, but probably none of the 11 closest matches at <5 arcsec. We can explore this further by making an object-by-object search through other catalogues,[7] with outcomes as noted below.

In order to attempt to separate the likely AGN, the HMXBs (which will be in star-forming galaxies) and the LMXBs (in passive old galaxies), we use the individual GAMA spectra. In total, 27 of the 28 low-mass galaxies have spectra from which spectral (emission) line fits have been obtained. The remaining object (GAMA J022858.99–050447.6, with $M_r = -17.9$) does not have measurable Hα or [O III] λ5007 emission lines, so could be assigned to be passive, or at least quiescent (denoted P in Table 1). Its X-ray source would then likely be an LMXB (cf. Papadopoulou et al. 2016). The X-ray luminosity is $10^{40.2}$ erg s^{-1}, though, which may seem unlikely for an LMXB, as Gilfanov (2004) suggests an upper cut-off at about $10^{39.5}$ erg s^{-1}. Intriguingly, the quoted X-ray source position is only 1.8 arcsec from the centre of the GAMA galaxy, which would be unlikely for an unassociated background contaminant, but certainly compatible with a nuclear source, while the galaxy's mid-infrared W1-W2 colour is relatively red, so we should perhaps not rule out a low luminosity AGN (cf. Dickey et al. 2019).

Extending the classifications via the emission-line plots, it appears that among the emission-line galaxies we have no clear cases of AGN and up to 27 likely star-forming galaxies (if we include the nine galaxies with Hα and/or [O III] lines, but no BPT classification). The X-ray sources in these would be expected to be HMXBs. Of course, the objects with no BPT classification could alternatively still be weak-lined AGN (see e.g. Agostino & Salim 2019), though the mid-infrared galaxy colours do not support this.

Searching around the 28 objects, we find that in three cases there are known QSOs within 10 arcsec of the GAMA galaxy (and at positions consistent with the XXL source), so these can be discounted as background contaminants (labelled BQ in the classification column in Table 1). In addition, in two cases there are QSOs further than 10 arcsec from the GAMA position, but still within the error circle for the matched XXL source, which could therefore be consistent with matching either the GAMA galaxy or the QSO. We consider these, too, to be likely contaminants (BQ? in the table). All these have quite large separations between the GAMA and XXL positions ($s \geq 7.5$ arcsec), and the number found is clearly consistent with the earlier statistical estimate of AGN contaminants (around 4). In addition, two of the GAMA galaxies are close (less than 10 arcsec on the sky) to more luminous $z \simeq 0.15$ galaxies, so the XXL sources might be linked to those galaxies, not the lower z ones in our low-mass sample (see XXL paper XXVII). We label these two as BG? in the table. Removing all seven likely or possible contaminants,[8] all of which have $s > 5$ arcsec, then leaves us with 20 likely genuine matched low-mass emission-line objects (though alternate matches may still exist for a few of them, cf. XXL paper XXVII).

The X-ray sources matched to these 20 emission-line galaxies lie in the range $L_{Xs} = 10^{39.2}$ to $10^{41.1}$ erg s^{-1}. The highest X-ray luminosities appear to (just) fit in the expected range, which cuts off at $\sim 10^{41}$ erg s^{-1} (e.g. Mineo et al. 2012) if the extension of HMXBs into ULXs is included.

In total, then, a reasonable number, $\simeq$20, likely XRBs have been found, probably mostly HMXBs in low-mass star-forming galaxies. For these, there is no correlation between X-ray luminosity and emission-line luminosity, which can easily be explained if the X-rays are from individual single HMXBs while the line emission reflects the ISM conditions and star formation in the galaxy.

It is difficult to relate our present results to those in the literature on the prevalence of HMXBs in brighter/more massive star-forming galaxies, for a number of reasons. In particular, we are able to detect only the brightest X-ray sources and have a flux limited rather than volume limited sample. Our nearest and faintest source is at $10^{39.2}$ erg s^{-1} while at the redshift of our most distant matched low-mass galaxy ($z \simeq 0.1$) the detection limit is approaching 10^{41} erg s^{-1}.

This can be contrasted with, for example, the general study of local star-forming galaxies by Mineo et al. (2012) who found about one HMXB for every 0.3 $M_\odot$ yr^{-1} of star formation, but with a detection limit 10^{38} erg s^{-1}, considerably below our accessible limits. Using a reasonable slope of the HMXB luminosity function (e.g. Grimm et al. 2003), we would need to correct the numbers detected in even nearby redshift bins (say at $z \simeq 0.03$, where the effective limit is around $10^{39.5}$ erg s^{-1}) by an order of magnitude, and in our more distant bins we are in the tail of the LF, near the upper cut-off, requiring very large (around two orders of magnitude) and very uncertain corrections. The best we can probably say is that, given our 20 actual detections, we would expect perhaps of order 500 detections if we had a similar X-ray limit to Mineo et al.

In addition, the intercomparison of SFRs is problematic: translating Hα luminosities to total SFRs (e.g. Kennicutt 1994) involves numerous uncertain steps (e.g. use of a particular initial mass function) and Mineo et al. (2012) use a completely different method based on infrared and ultraviolet luminosities. If, for a concrete example, we simply translate Hα luminosity to an 'indicative' SFR via Kennicutt (1983)'s relation SFR $\simeq L_{\mathrm{H}\alpha}/(10^{41}$ erg s^{-1}) $M_\odot$ yr^{-1},

[7]From ned.ipac.caltech.edu, skyserver.sdss.org/dr7/, and SIMBAD.

[8]The mismatch between a BPT classification as SF and an association with a QSO/AGN is not relevant regarding the contaminants, as in each case the QSO/AGN is outside the area of the fibre used for the GAMA spectroscopy.

ignoring any systematics in this translation,[9] then the total indicative SFR summed over our 21 low-mass host galaxies (we exclude those where the X-ray source is probably associated with a background AGN or a different galaxy) is about 4 $M_\odot\,yr^{-1}$ (see the middle panel of Fig. 9).

However, our final low-mass matched sample of objects is only about 2 per cent of the total number of GAMA galaxies fainter than $M_R = -19$ in the XXL overlap region; as expected the very large majority of nearby low-mass galaxies have no detectable HMXBs down to our (rather high) X-ray luminosity limits (cf. Gilfanov, Grimm & Sunyaev 2004). Calculating the SFR in the same way for the whole set of low luminosity GAMA galaxies, we obtain about 220 $M_\odot\,yr^{-1}$, i.e. approximately 1 detection per 10 $M_\odot\,yr^{-1}$ of indicative SFR. (Note that the average SFRs in the X-ray detected and non-X-ray detected low-mass galaxies are very similar, $\sim 0.2\,M_\odot\,yr^{-1}$.) With our above very rough estimate of 500 putative detections if we could observe uniformly down to $10^{38}\,erg\,s^{-1}$, we nominally obtain one 'detection' per $0.4\,M_\odot\,yr^{-1}$, i.e. of the same order of magnitude as that (really) seen in bright galaxies. Of course, here we are implicitly assuming that the HMXB LF is similar in high-mass and low-mass galaxies and that we can ignore any systematic corrections to our derived Hα based SFRs.

One might think that a way to avoid the latter systematics would be to make an internal comparison to our brighter, more massive, GAMA galaxies, using the same SFR recipe. However, these galaxies have typical SFR $\simeq 1\,M_\odot\,yr^{-1}$, so on the Mineo et al. scale should generally have multiple HMXBs, which would most likely be recorded as a single, potentially much brighter, source at the spatial resolution of the XXL survey. Hence, we could seriously undercount sources originating in the high-mass galaxies.

Nevertheless, in the spirit of our order of magnitude calculations, we can reverse the above argument and estimate that for luminosity limits of $10^{39.5}$ to $10^{41}\,erg\,s^{-1}$, as appropriate to our sample, Mineo et al. would have seen about 0.1 to 0.01 (rather than 1) sources per $0.3\,M_\odot\,yr^{-1}$, depending on the source distance. Looking at the sample of 1200 $z < 0.1$ optically bright ('high mass') galaxies, with $M_R < -19$, in our GAMA/XXL overlap region, 965 have measurable lines with a total indicative SFR of $1150\,M_\odot\,yr^{-1}$. This would imply somewhere of order 100 detectably bright sources. In fact, 148 of the low-redshift galaxies are sufficiently bright in X-rays to be detected in our sample (see Fig. 3), presumably including some low-z AGN.

Finally, if we simply compare the total X-ray luminosity from our low-mass sample, roughly $7 \times 10^{41}\,erg\,s^{-1}$, to the total star formation rate from all the low-mass galaxies in our area, $220\,M_\odot\,yr^{-1}$, we get a ratio of around $3 \times 10^{39}\,erg\,s^{-1}$ per 1 $M_\odot\,yr^{-1}$. This is in reasonable agreement with the ratio 5×10^{39} given by Ranalli et al. (2003) for more massive galaxies, given that we have necessarily underestimated the total X-ray flux from the full set of low-mass galaxies (non-detections may have low-level flux).

From all these arguments, we therefore conclude that there is no strong evidence that the number of bright HMXBs per unit of star formation is substantially different in low-mass galaxies compared to high-mass galaxies (cf. Papadopoulou et al. 2016). Equally, of course, we can make no strong claims that it is indeed the same.

[9]Such as the fraction of Hα flux missed from outside the aperture of the GAMA spectra.

If we take the BPT classifications at face value, then we have no definite AGN. If, instead, we argue, for instance, that the signature of low-mass SMBH can be drowned by that of coexisting star formation (e.g. Baldassare, Geha & Greene 2018), so that we should not rely too much on the BPT plot (and since not all our objects have BPT classifications), we could consider sources apparently at small galactocentric distances and/or with particularly high L_{Xs} as potential AGNs. We already noted the one passive galaxy in the sample in this regard. Among the emission-line objects, 10 have $s < 5$ arcsec, 6 of them with positional separations less than 3 arcsec. Five of the latter are classified star-forming (SF in Table 1) and one has no classification. All six have low [O III] luminosities for an AGN, none exceeding $10^{40.3}\,erg\,s^{-1}$ (cf. Gordon et al. 2017). There are two sources with X-ray luminosities $L_{Xs} \geq 10^{41}\,erg\,s^{-1}$, considered high for an HMXB. One is at a separation of 4.5 arcsec and is classed as SF and one, at $s = 8.9$ arcsec, is unclassified.

We could then have as many as nine candidate AGNs from sources that are either close to the centre of the galaxy (including the passive galaxy) or of higher than expected X-ray luminosity for an XRB. However, the failure of the reverse criteria in each case (not bright enough or not central enough, except possibly in one case) renders these unlikely AGNs even without the BPT results and the galaxy-like mid-infrared colours.

Thus, in agreement with previous work, (X-ray) AGNs in low-mass galaxies remain difficult to detect, even when we have complete samples of tens of thousands of both X-ray sources (from XXL) and galaxies (from GAMA), albeit flux-limited samples in each case, rather than volume-limited samples. Regardless of that caveat, we find no convincing AGN in the 1200 low-mass galaxies sampled in the overlap region.

To see how many we might have expected, we can make a very simple argument. If the X-ray luminosity is proportional to the black hole mass and that in turn is a given fraction of the host galaxy stellar mass, then the X-ray luminosity should be proportional to the optical luminosity. Thus, the ratio of the X-ray flux to optical flux should not depend on the optical luminosity. In other words, a 19^m galaxy, for instance, should have the same X-ray flux, and therefore be equally detectable, regardless of whether it is a nearby dwarf or a distant giant. As we detect about 800 GAMA galaxies in X-rays, or 4 per cent of the 20 000 galaxies in the overlap region, then all other things being equal, and assuming most of the sources in massive galaxies are AGNs (Yao et al. 2020), we should also expect 4 per cent of the 1200 low-mass galaxies to be X-ray detectable AGNs, i.e. about 50.

Clearly this is not the case, so we can conclude that our simple model breaks down; that is, one or more of the proportionalities assumed are different for low-mass and high-mass galaxies. For instance, if the black hole mass is in fact proportional to the bulge, rather than total, mass (Ferrarese et al. 2006a) and low-mass galaxies are mostly disc-dominated systems with small (or even negligible) bulge fractions (e.g. Moffett et al. 2016), then we might expect lower black hole masses compared to the case of simply scaling down giant galaxies (see also Koliopanos et al. 2017; Baldassare et al. 2018; Davis, Graham & Cameron 2018). Alternatively (or additionally), it may be that the distribution of Eddington ratios is different (on average lower) for low-mass galaxies that will typically have lower central densities (Fang et al. 2013), perhaps reducing mass infall into the black hole. Finally, it may be that the black hole occupation fraction is low in these galaxies (for a summary of observed occupation fractions, see Mezcua 2017).

ACKNOWLEDGEMENTS

GAMA is a joint European–Australasian project based around a spectroscopic campaign using the Anglo-Australian Telescope. The GAMA input catalogue is based on data taken from the Sloan Digital Sky Survey and the UKIRT Infrared Deep Sky Survey. Complementary imaging of the GAMA regions is being obtained by a number of independent survey programmes including *GALEX* MIS, VST KiDS, VISTA VIKING, *WISE*, *Herschel*-ATLAS, GMRT, and ASKAP, providing UV to radio coverage. GAMA is funded by the Science and Technology Facilities Council (STFC; UK), the Australian Research Council(ARC) (Australia), the Australian Astronomical Observatory (AAO), and the participating institutions. The GAMA website is http://www.gama-survey.org/. XXL is an international project based around an XMM Very Large Programme surveying two 25 deg^2 extragalactic fields in the [0.5–2.0] keV band for point-like sources. It is based on observations obtained with *XMM–Newton*, an European Space Agency (ESA) science mission with instruments and contributions directly funded by ESA Member States and National Aeronautics and Space Administration (NASA). The XXL website is http://irfu.cea.fr/xxl. Multiwavelength information and spectroscopic follow-up of the X-ray sources are obtained through a number of survey programmes, summarized at http://xxlmultiwave.pbworks.com/. During the course of the initial part of this work, EN was supported by a scholarship from the Nigerian Tertiary Education Trust Fund. The Bristol Alumni Fund is also thanked for their additional support. AE acknowledges support from the budgetary programme of the National Academy of Science(NAS) of Ukraine 'Support for the development of priority fields of scientific research' (CPCEL 6541230). MP acknowledges long-term support from the Centre National d'Etudes Spatial (CNES). This work made extensive use of TOPCAT (Taylor 2005) software packages, which are supported by an STFC grant to the University of Bristol. The authors thank the referee for useful comments.

DATA AVAILABILITY

The data underlying this paper are available at http://www.gama-survey.org/dr3/ and/or are available in the article.

REFERENCES

Abazajian K. N. et al., 2009, ApJS, 182, 543
Adelman-McCarthy J. K. et al., 2008, ApJS, 175, 297
Agostino C. S., Salim S., 2019, ApJ, 876, 12
Aihara H. et al., 2011, ApJS, 193, 29
Alexander D., Hickox R., 2012, New Astron. Rev., 56, 93
Baldassare V. F., Reines A. E., Gallo E., Greene J. E., 2017, ApJ, 836, 20
Baldassare V. F., Geha M., Greene J., 2018, ApJ, 868, 152
Baldassare V. F., Dickey C., Geha M., Reines A. E., 2020, ApJ, 898, 3
Baldry I. K. et al., 2010, MNRAS, 404, 86
Baldry I. K. et al., 2012, MNRAS, 421, 621
Baldry I. K. et al., 2018, MNRAS, 474, 3875
Baldwin J. A., Phillips M. M., Terlevich R., 1981, PASP, 93, 5
Bell E. F., McIntosh D. H., Katz N., Weinberg M. D., 2003, ApJS, 149, 289
Boroson B., Kim D.-W., Fabbiano G., 2011, ApJ, 729, 12
Chiappetti L. et al., 2018, A&A, 620, 12 (XXL paper XXVII)
Cluver M. E. et al., 2014, ApJ, 782, 90
Crossett J. P. et al., 2021, A&A, to be submitted
Davis B. L., Graham A. W., Cameron E., 2018, ApJ, 869, 113
Decarli R., Gavazzi G., Arosio I., Cortese L., Boselli A., Bonfanti C., Colpi M., 2007, MNRAS, 381, 136
Dickey C. M., Geha M., Wetzel A., Al-Badry K., 2019, ApJ, 884, 180
Driver S. P. et al., 2011, MNRAS, 413, 971
Dudik R. P., Satyapal S., O'Halloran B., Watson D., 2005, ApJ, 620, 113
Fang J. J., Faber S. M., Koo D. C., Dekel A., 2013, ApJ, 776, 63
Ferrarese L. et al., 2006a, ApJ, 644, L21
Ferrarese L. et al., 2006b, ApJS, 164, 334
Fotopoulou S. et al., 2016a, A&A, 587, 142
Fotopoulou S. et al., 2016b, A&A, 592, A5 (XXL paper VI)
Gallo E., Treu T., Jacob J., Woo J.-H., Marshall P. J., Antonucci R., 2008, ApJ, 680, 154
Giles P. A. et al., 2021, A&A, to be submitted
Gilfanov M., 2004, MNRAS, 349, 146
Gilfanov M., Grimm H.-J., Sunyaev R., 2004, MNRAS, 351, 1365
Gordon Y. A. et al., 2017, MNRAS, 465, 2671
Graham A. W., Driver S. P., 2005, Publ. Astron. Soc. Aust., 22, 118
Greene J. E., Ho L. C., 2007, ApJ, 667, 131
Grimm H. J., Gilfanov M., Sunyaev R., 2003, MNRAS, 339, 793
Grisé F., Kaaret P., Pakull M. W., Motch C., 2011, ApJ, 734, 23
Gwyn S. D. J., 2012, AJ, 143, 38
Hainline K. N., Reines A. E., Greene J. E., Stern D., 2016, ApJ, 832, 119
Heckman T.M, Ptak A., Hornschemeier A., Kauffmann G., 2005, ApJ, 634, 161
Heymans C. et al., 2012, MNRAS, 427, 146
Ho L. C., 2008, ARA&A, 46, 475
Hopkins A. M. et al., 2013, MNRAS, 430, 2047
Jarrett T. H. et al., 2011, ApJ, 735, 112
Kauffmann G. et al., 2003, MNRAS, 341, 33
Kauffmann G. et al., 2003, MNRAS, 346, 1055
Kennicutt R. C., 1983, ApJ, 272, 54
Kennicutt R. C., 1992, ApJ, 388, 310
Kennicutt R. C., Tamblyn P., Congdon C. E., 1994, ApJ, 435, 22
Kewley L., Dopita M. A., Sutherland R. S., Heisler C. A., Trevena J., ApJ, 556, 121
Koliopanos F. et al., 2017, A&A, 601, 20
Koulouridis E. et al., 2018, A&A, 620, 4 (XXL paper XIX)
Lange R. et al., 2015, MNRAS, 447, 2603
Lange R. et al., 2016, MNRAS, 462, 1470
Lewis I. J. et al., 2002, MNRAS, 333, 279
Liske J. et al., 2015, MNRAS, 452, 2087
Magorrian J. et al., 1998, AJ, 115, 2285
Mezcua M., 2017, Int. J. Mod. Phys. D, 26, 1730021
Mezcua M., Civano F., Marchesi S., Suh H., Fabbiano G., Volonteri M., 2018, MNRAS, 478, 2576
Miller C. J. et al., 2003, ApJ, 271, L7
Mineo S., Gilfanov M., Sunyaev R., 2012, MNRAS, 419, 2095
Moffett A. J. et al., 2016, MNRAS, 457, 1308
Mulchaey J. S., KoratkurA., Ward M. J., Wilson A. S., Whittle M., Antonucci R. R. J., Kinney A. L., Hurt T., 1994, ApJ, 436, 586
Pacaud F. et al., 2016, A&A, 592, 2 (XXL paper II)
Panessa F., Bassani L., Cappi M., Dadina M., Barcons X., Carrera F. J., Ho L. C., Iwasawa K., 2006, A&A, 455, 173
Papadopoulou M., Phillipps S., Young A. J., 2016, MNRAS, 460, 4513
Pardo K. et al., 2016, ApJ, 831, 203
Pierre M. et al., 2016, A&A, 592, A11 (XXL paper I)
Pineau F.-X. et al., 2011, A&A, 527, 126
Ranalli P., Comastri A, Setti G., 2003, A&A, 399, 39
Reines A. E., Greene J. E., Geha M., 2013, ApJ, 775, 116
Robotham A. et al., 2010, Publ. Astron. Soc. Aust., 27, 76
Robotham A. et al., 2011, MNRAS, 416, 2640
Saunders W. et al., 2004, in Moorwood A. F. M., Masanori I., eds, Proc. SPIE Conf. Ser. Vol. 5492, Ground-Based Instrumentation for Astronomy. SPIE, Bellingham, p. 389
Seth A., Agueros M., Lee D., Basu-Zych A., 2008, ApJ, 678, 116
Sharp R. et al., 2006, in McLean I. S., Masanori I., eds, Proc. SPIE Conf. Ser. Vol. 6269, Ground-Based and Airborne Instrumentation for Astronomy. SPIE, Bellingham, p. 62690G

Stern D. et al., 2012, ApJ, 753, 30
Sutton A. D., Roberts T. P., Walton D. J., Gladstone J. C., Scott A. E., 2012, MNRAS, 423, 1154
Swartz D. A., Soria R., Tennant A. F., Yukita M., 2011, ApJ, 741, 49
Taylor M. B., 2005, in Shopbell P., Britton M., Ebert R., eds, ASP Conf. Ser. Vol. 347, Astronomical Data Analysis Software and Systems XIV. Astron. Soc. Pac., San Francisco, p. 29
van der Wel A. et al., 2014, ApJ., 788, 28
Woods T. E. et al., 2019, Publ. Astron. Soc. Aust., 36, e027
Yao H. F. M. et al., 2020, ApJ, 903, 91

This paper has been typeset from a TEX/LATEX file prepared by the author.